The following supplement accompanies the article

Tidal and subtidal currents influence deep copepod aggregations along a shelf-basin margin

Kimberley T. A. Davies*, Tetjana Ross, Christopher T. Taggart

Department of Oceanography, Dalhousie University, 1355 Oxford Street, Halifax, Nova Scotia B3H4R2, Canada

*Email: kim.davies@dal.ca

Marine Ecology Progress Series 000: 000–000 (2013)

Supplement. Relative zooplankton concentration estimation

Relative zooplankton concentrations (S) were estimated for each beam using an RDI-specific form of the sonar equation (Deines 1999):

$$S\,(z,t) = C + 10\log_{10}((\,T_x + 273.16)\,R^2\,) - L_{DBM} - P_{DBW} + 2\alpha R + K_C\,(E - E_r\,) - TS \qquad \text{(S1)}$$

where $S(z,t)$ is relative zooplankton concentration (dB) at each depth z and time step t, TS is the frequency-specific target strength of the dominant sound scatterers, C is a 'typical value' for a factory estimated calibration coefficient (–141.4, see Table 1 in Deines 1999), T_x is transducer temperature (6°C), R is slant range (m), L_{DBM} is 10 × $\log_{10}$(transmit pulse length, 4.3297 m), P_{DBW} is 20 × $\log_{10}$(transmit power, varied in time), α is the frequency-specific absorption coefficient of water (0.0809, 0.1643, and 0.3557 dB m^{-1} for the 300, 600, and 1000 kHz instruments, respectively), E is echo intensity, E_r is the factory measured real-time reference level for the echo intensity (range: 42–50 counts), and K_c is a factory measured beam-specific constant that converts E to units of dB (range: 0.3833–0.4230 dB $count^{-1}$). Note that because C is a typical value for instruments of our model and frequency, and was not estimated for our instruments specifically, it is possible that the absolute values of $S\,(z,t)$ will not be in the range typically expected for zooplankton concentrations. Hence, the values of $S\,(z,t)$ are only interpretable in relative terms. We expect S (z,t) to vary by approximately 10 dB over time within the zooplankton layer based on the concentrations in nets (100–1000 m^{-3}, see Tables S2–S5), which is similar to the range measured by the ADCPs (Fig. S1). $S\,(z,t)$ was then converted into linear space using s $(z,t) = 10^{S(z,t)/10}$. Units of $s\,(z,t)$ are the number of dominant scatterers m^{-3}. The linear metric was used for the remainder of the manuscript.

Ten of the BIONESS nets collected zooplankton samples in the focal depth layer, between 75 and 150 m (see Tables S2–S5). C*alanus finmarchicus* stage C5 and *C. hyperboreus* stage C4 (hereafter CF5 and CH4, respectively) were the most abundant organisms in the nets. Other potentially important scatterers such as euphausiids were rarely collected (see Tables S2–S5), and the lack of diel-vertical migration evident in the acoustic backscatter (S; Fig. S1) suggested that backscatter from such organisms was minimal at the mooring locations. Using the abundance (from net-samples) and size frequency (from net-samples or literature) data for all the zooplankton taxa caught in the nets, and standard weak-scattering models for zooplankton (e.g. Lavery et al. 2007), we found that within the focal layer, 86 ± 12% (SD, n = 11), 82 ± 18%, and 85 ± 12% of acoustic scattering at the 300, 600, and 1000 kHz frequencies, respectively, was due to a combination of CF5s and CH4s (Figs. S2–S4). Other scatterers, particularly ctenophores, were dominant scatterers in the depth-integrated nets. Since ctenophores were absent in the deep nets from the same locations, it is likely that these scatterers were in the upper water column and well away from the diapausing copepod layer.

The size distributions of CF5s and CH4s were combined, scaled for relative concentration, and used to estimate the average frequency-specific target strength (*TS*) of a 'typical copepod' needed for Eq. (S1), using the Distorted Wave Born Approximation (DWBA) model for copepods developed by Stanton & Chu (2000; Fig. S5). The density (g) and sound speed (h) contrast parameters used were 1.02 and 1.058, respectively. Target strengths were −103.1, −102.9, and −103.7 dB for the 300, 600, and 1000 kHz instruments (Fig. S5).

Problems estimating the vertical velocities

At each mooring, horizontal currents measured by the upward-looking RDI acoustic Dopper current profiler (ADCP) and the downward-looking Aquadopp ADCP were in good agreement (Figs. S3 & S4). The vertical velocities ($W(z,t)$) however, did not agree between the 2 instruments at either mooring. The patterns were similar between instruments, but the RDIs always measured larger positive $W(z,t)$ than the Aquadopps. On average, the RDIs measured deep-basin (>60 m) velocities that were positive, and the Aquadopps measured near-bottom velocities that were negative; however, Aquadopp $W(z_{min},t) \neq -1 \times$ *RDI* $W(z_{max},t)$). The reasons for this disagreement are unclear. It is possible, although it seems unlikely, that we measured real changes in $W(z,t)$ with depth and that the transition zone between positive and negative velocities occurred within our 4 m blanking region around stream-lined underwater buoyancy system (SUBS) units at both moorings. However, $W(z,t)$ did not decrease with depth above or below the blanking region to suggest such a transition; the change was abrupt. More likely, the disagreement resulted from a technical issue. The magnitudes of $W(z,t)$ from all instruments were larger than the error velocities, meaning that the variation measured in $W(z,t)$ was not simply due to background noise. If the ADCPs were not oriented with the center axis perfectly perpendicular to the seafloor and ocean surface, which could happen if the SUBS units were unbalanced, then some of the variation in the horizontal currents could instead be measured as vertical currents. In that case, we might expect (1) vertical currents to be abnormally large in amplitude, because horizontal currents are 1 to 2 orders of magnitude larger in amplitude than vertical currents, and (2) high correlation between the horizontal and vertical currents. The vertical currents we measured were not abnormally large on any instrument, averaging ±3 mm s^{-1} at depth and reaching a maximum of ~2 cm s^{-1}. Horizontal and vertical currents were also not well correlated ($r < 0.3$) at any depth for either instrument at the shallow-slope mooring or for the Aquadopp at the deep-slope mooring. Horizontal and vertical currents near the transducer of the deep-slope RDI were better correlated ($r = 0.43$), and this correlation declined with distance from the transducers. In summary, we are uncertain which instruments (if either), the Aquadopps or the RDIs, measured the vertical current magnitudes correctly.

Thermal wind calculation

We used a section of the density field estimated in the cross-isobath direction near our ADCPs (Fig. S8) and the equation for thermal wind (Eq. S2) to approximate the magnitude of the along-isobath velocity (v) generated by baroclinicity on the southeastern margin of the basin. We made this calculation at 75, 100, and 125 m depths, assuming a level of no motion at 150 m depth,

$$\frac{\Delta v}{\Delta z} = -\frac{g}{\rho f}\frac{\Delta \rho}{\Delta x} \qquad \text{(S2)}$$

where z is depth (m), g is the acceleration due to gravity, f is the Coriolis coefficient, ρ is average water column density, and $\frac{d\rho}{dx}$ is the horizontal change in density in a cross-isobath (x) direction between 15 and 20 km along the transect. The data region is depicted by a black box in Fig. S8. An example calculation made at 125 m depth is provided below. We estimate $v_{125} = 2$ cm s^{-1}, $v_{100} = 4$ cm s^{-1}, and $v_{75} = 0$ cm s^{-1}.

ρ = 1025.9 kg m^{-3} (estimated from Fig. S8)
g = $^{-}$10 m s^{-2}
f (45° latitude) = 10^{-4} s^{-1}
$\frac{\Delta\rho}{\Delta x} = \frac{0.04\ \mathrm{kg\ m^{-3}}}{5000\ \mathrm{m}}$ (estimated from Fig. S8)
$\Delta z = -150\mathrm{m} - (-125\ \mathrm{m}) = -25\ \mathrm{m}$
$\Delta v = v_{150\ \mathrm{m}} - v_{125\ \mathrm{m}}$
$v_{150\ \mathrm{m}} = 0\ \mathrm{m\ s^{-1}}$ (assuming a level of no motion at 150 m depth)

$$\frac{0 - v_{125\ \mathrm{m}}}{-25\ \mathrm{m}} = -\frac{-10\ \mathrm{m\ s^{-2}}}{(1025.9\ \mathrm{kg\ m^{-3}})(10^{-4} s^{-1})} \times \frac{0.04\ \mathrm{kg\ m^{-3}}}{5000\ \mathrm{m}}$$

v_{125} = + 0.02 m s^{-1} (into the page, toward the northeast)

Table S1. Summary characteristics of each station sampled using BIONESS in Roseway Basin during 4 through 13 September 2008. Provided are the number of nets deployed, start dates and time (Atlantic Daylight Time), latitude and longitude locations, and maximum sampling depth. Net-specific data are provided in Tables S2–S5

Station	No. of nets	Start date (mm/dd)	Start time (h)	Start lat (°N)	Start long (°W)	Max depth (m)
B01	5	09/05	12:40	42.560	65.020	135
B02	5	09/06	09:40	43.276	65.392	150
B03	2	09/12	23:55	42.507	65.136	143
B04	6	09/13	12:27	42.539	65.876	147

Table S2. Zooplankton species assemblage and concentrations (ind. m^{-3}) in 2008 collected with BIONESS at Stn B01, Roseway Basin. Values are given for samples from depth-integrated nets (first column) and depth-specific (depth interval) nets. F: female, M: male

	Tow depth interval (m)				
Species	0–135	120–135	110–120	90–110	0–90
Mesozooplankton:					
Calanus finmarchicus C3	3	0	0.4	0	0.3
Calanus finmarchicus C4	13	0.5	1	0	2
Calanus finmarchicus C5	25	14	78	131	19
Calanus finmarchicus F	4	1	8	8	0.3
Calanus finmarchicus M	0.9	1	4	0.7	0
Calanus hyperboreus	7	7	19	33	0
Calanus glacialis	0	0.4	3	1	0
Metridia spp.	0	1	6	4	0
Centropages spp.	38	0	0.4	0.7	21
Pseudocalanus spp.	7	3	3	0.7	4
Paracalanus spp.	4	16	41	7	0.3
Oithonia spp.	0	0	0	0	0
Temora spp.	0	0	0	0	0
Amphipoda	4	0.1	0	0.7	1
Ctenophora	13	2	0.4	0	0
Ostracoda	0	0	0	0	0
Cladocera	0	0	0	0	0
Euchaeta spp.	0	0	0	0	0

Gastropoda	0	0	0	0	0
Euphausiidae (<2 cm)	0	0	0	1	0.5
Total mesozooplankton	119	45	163	188	47
Macrozooplankton:					
Euphausiidae (>2 cm)	0	0	0	0	0.01
Amphipoda	0	0	0	0	0.05
Ctenophora	0	0	0	0	0.02
Total macrozooplankton	0	0	0	0	0.08

Table S3. Zooplankton species assemblage and concentrations (ind. m^{-3}) in 2008 collected with BIONESS at Stn B02, Roseway Basin. Values are given for samples from depth-integrated nets (first column) and the deep-sampling (144–150 m) nets. F: female, M: male

	Tow Depth Interval (m)				
Species	0–144	144–146	146–148	148–150	150–150
Mesozooplankton:					
Calanus finmarchicus C3	0	0	0	2	0
Calanus finmarchicus C4	2	2	2	1	2
Calanus finmarchicus C5	262	396	344	427	707
Calanus finmarchicus F	5	16	25	15	19
Calanus finmarchicus M	3	0	0	2	0
Calanus hyperboreus	131	223	130	151	256
Calanus glacialis	10	6	2	14	33
Metridia spp.	2	2	2	9	8
Centropages spp.	12	2	0	0	0
Pseudocalanus spp.	0	2	2	2	4
Paracalanus spp.	5	10	8	1	5
Oithonia spp.	0	0	0	0	0
Temora spp.	0	0	0	0	0
Amphipoda	5	0	0	0	0
Ctenophora	29	0	0	0	0
Ostracoda	2	0	0	0	0
Cladocera	0	0	0	0	0
Euchaeta spp.	0	0	0	0	0
Gastropoda	0	0	2	0	0
Euphausiidae (<2 cm)	0	0	0	0	0
Total mesozooplankton	468	660	517	623	1035
Macrozooplankton:					
Euphausiidae (>2 cm)	0	0	0	0	0
Amphipoda	0	0	0	0	0
Ctenophora	0	0	0	0	0
Total macrozooplankton	0	0	0	0	0

Table S4. Depth-integrated zooplankton species assemblage and concentrations (ind. m^{-3}) collected with BIONESS at Stn B03 in 2008 in Roseway Basin. F: female, M: male

Species	Tow depth interval (m)	
	0–143	0–143
Mesozooplankton:		
Calanus finmarchicus C3	0.6	0
Calanus finmarchicus C4	6	11
Calanus finmarchicus C5	371	901
Calanus finmarchicus F	11	5
Calanus finmarchicus M	2	2
Calanus hyperboreus	96	202
Calanus glacialis	26	73
Metridia spp.	12	13
Centropages spp.	29	24
Pseudocalanus spp.	6	0
Paracalanus spp.	2	2
Oithonia spp.	0.6	2
Temora spp.	0.6	0
Amphipoda	1	2
Ctenophora	0	9
Ostracoda	0	0
Cladocera	0	0
Euchaeta spp.	0	0
Gastropoda	0	0
Euphausiidae (<2 cm)	0	0
Total mesozooplankton	565	1246
Macrozooplankton:		
Euphausiidae (>2 cm)	0	0.01
Amphipoda	0	0
Ctenophora	0	0
Total macrozooplankton	0	0.01

Table S5. Zooplankton species assemblage and concentrations (ind. m^{-3}) in 2008 collected with BIONESS at Stn B04, Roseway Basin. Values are given for samples from depth-integrated nets (first column) and specific (depth interval) nets. F: female, M: male

	Tow Depth Interval (m)					
Species	0–47	147–147	139–147	75–139	50–75	0–50
Mesozooplankton:						
Calanus finmarchicus C3	0.7	0	0	0	0	0
Calanus finmarchicus C4	0.7	18	23	2	0.3	8
Calanus finmarchicus C5	57	1130	475	99	8	42
Calanus finmarchicus F	5	3	5	3	0.6	5
Calanus finmarchicus M	2	2	3	2	0.1	1
Calanus hyperboreus	20	70	126	16	0.3	0.7
Calanus glacialis	5	2	0	0	0	0
Metridia spp.	6	15	19	4	0.3	1
Centropages spp.	7	2	0	0	0.8	84
Pseudocalanus spp.	0.7	5	5	2	0.7	14
Paracalanus spp.	1	4	13	11	0	8
Oithonia spp.	0	0	0	0	0	0
Temora spp.	0	0	0	0	0	0
Amphipoda	0	0	0	2	5	9
Ctenophora	152	0	0	0	0	0
Ostracoda	0	0	0	0	0	0
Cladocera	0	0	0	0	0	0
Euchaeta spp.	0	0	0	0	0	0
Gastropoda	0	0	0	0	0	0
Euphausiidae (<2 cm)	0	0	0	0.4	0.7	3
Total mesozooplankton	257	1251	669	141	18	176
Macrozooplankton:						
Euphausiidae (>2 cm)	0	0.007	0.004	0	0	0
Amphipoda	0	0	0	0	0	0
Ctenophora	0	0	0	0	0	0
Total macrozooplankton	0	0.007	0.004	0	0	0

Fig. S1. Time series of depth-specific relative plankton concentration (*S*, dB) collected with acoustic Doppler current profilers (ADCPs) at the (a) deep- and (b) shallow-slope moorings in Roseway Basin over day of year 249 through 257, 2008 (labels centered at 00:00 h ADST). The white horizontal bar in each sectional plot illustrates the 4 m blanking region between the upward- and downward-looking ADCPs. The black and white bar at the top of the plot indicates day (white) and night (black). Note: the absolute values of *S* are not expected to be within the range of scattering zooplankton (see above, Relative zooplankton concentration estimation); only the relative changes are interpretable

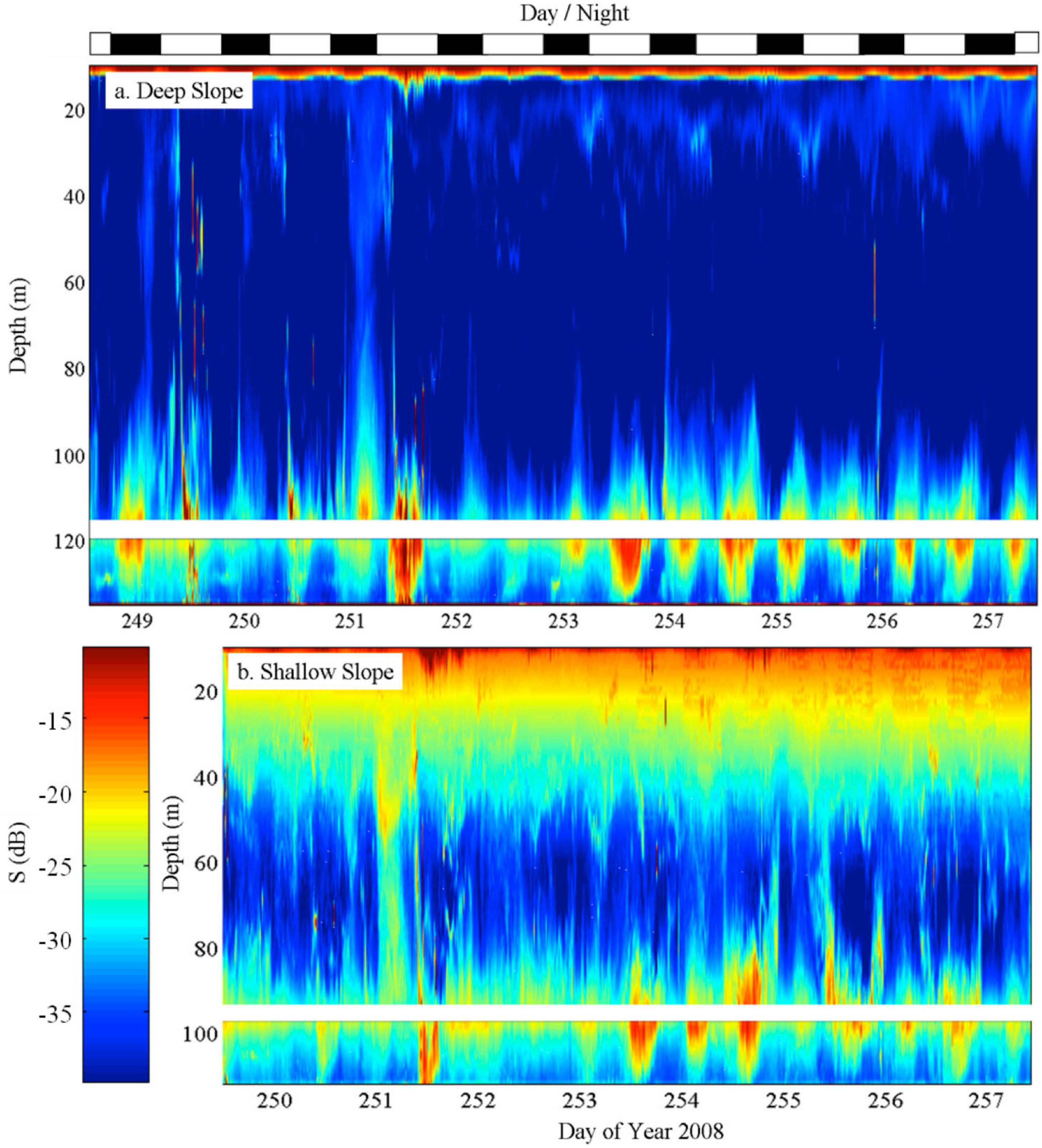

Fig. S2. Contribution to the total volume scattering (m^{-1}) at 300 kHz for scattering organisms collected in each BIONESS net, where the collection-depth interval of each net is provided on the abscissa along with BIONESS station numbers. At Stn B04, the depth integrated (0–147 m) sample contained scatterers with a total contribution that reached 4.9×10^{-7} m^{-1} (graphically limited to 1.3×10^{-7} m^{-1}). F: female, M: male

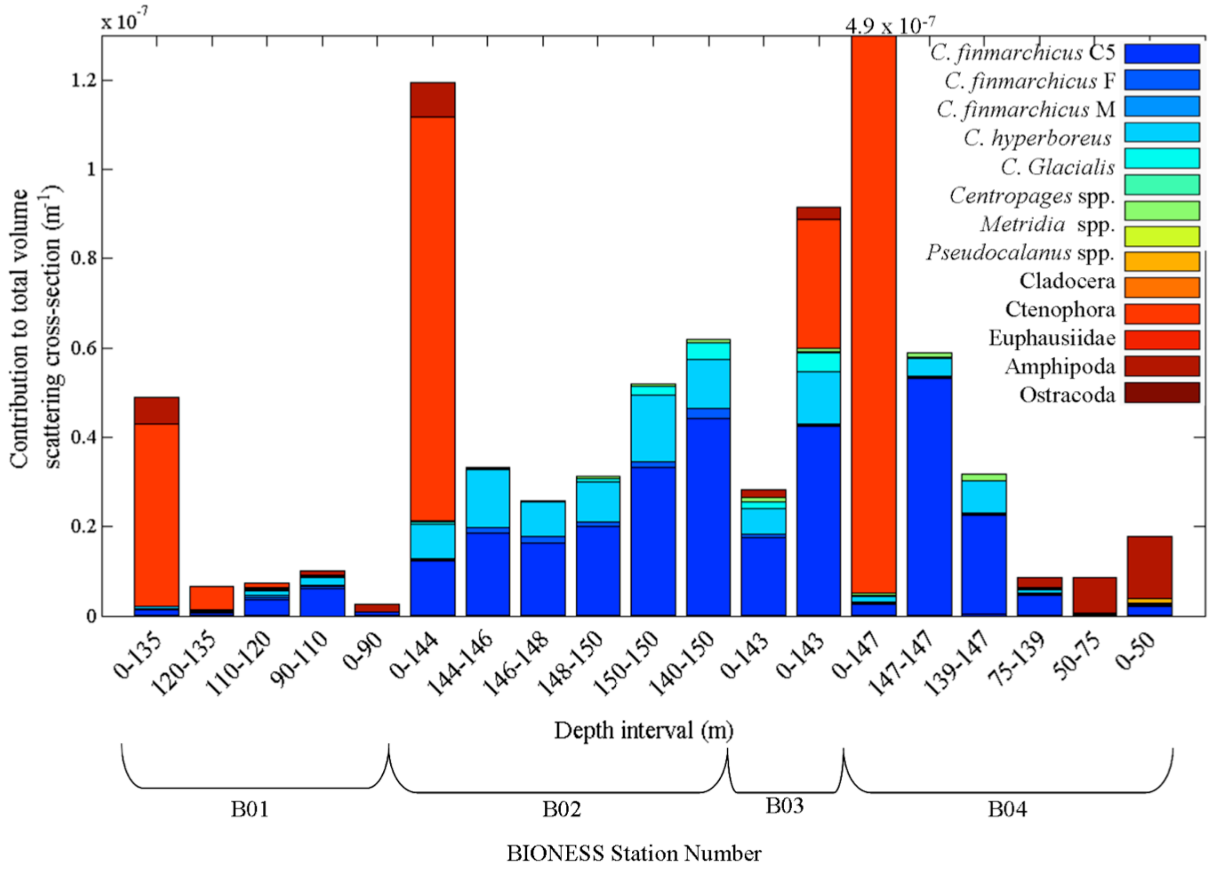

Fig. S3. As in Fig. S2, but for the 600 kHz frequency

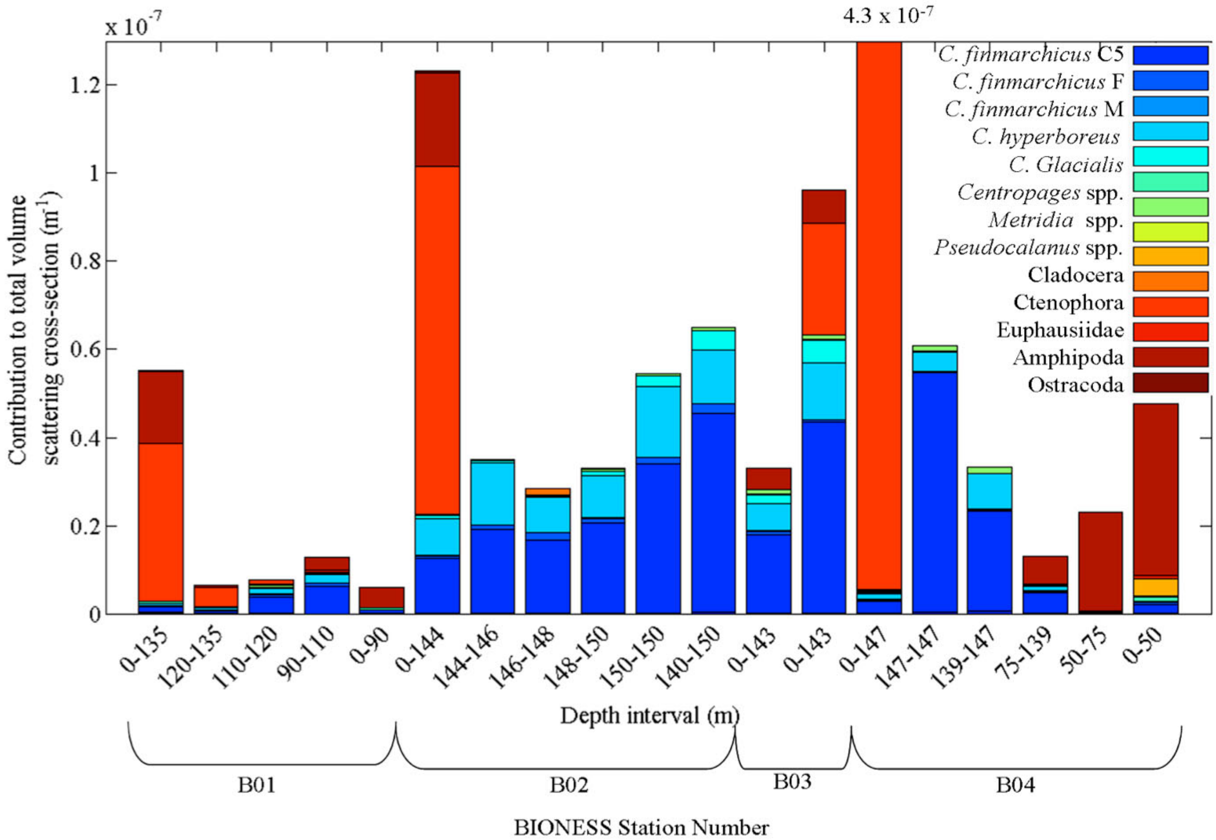

Fig. S4. As in Fig. S2, but for the 1000 kHz frequency

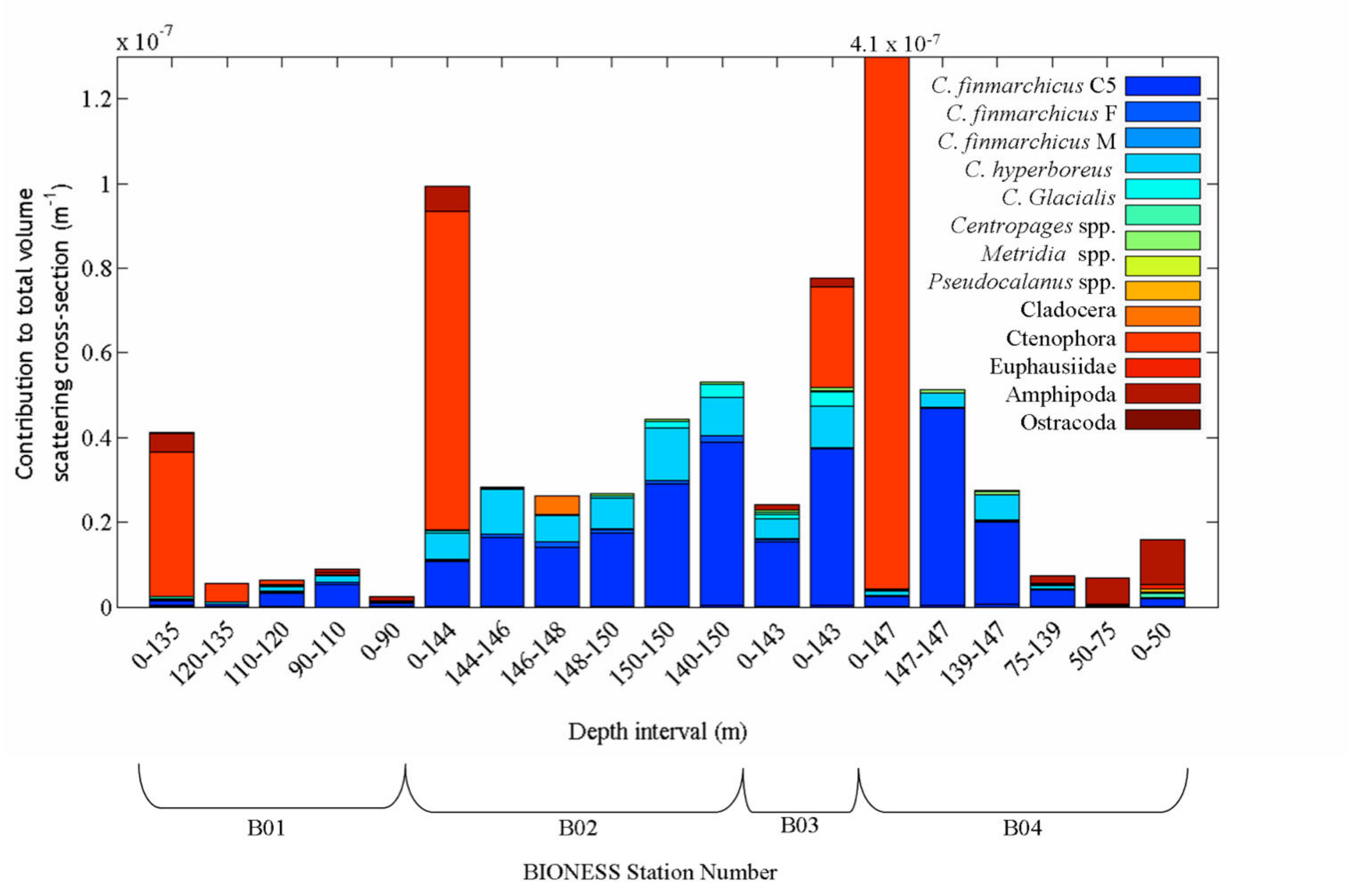

Fig. S5. Target strength (TS) frequency distribution for a 'typical copepod' estimated from the combined size distribution of *Calanus finmarchicus* C5 and *C. hyperboreus* C4, corrected for relative concentration of each species. Samples were collected in BIONESS nets below 90 m depth in Roseway Basin. Dots with horizontal blue bars : mean ± 95% CI target strengths for the beam frequency-specific (300, 600, and 1000 kHz) distributions. N = 1000

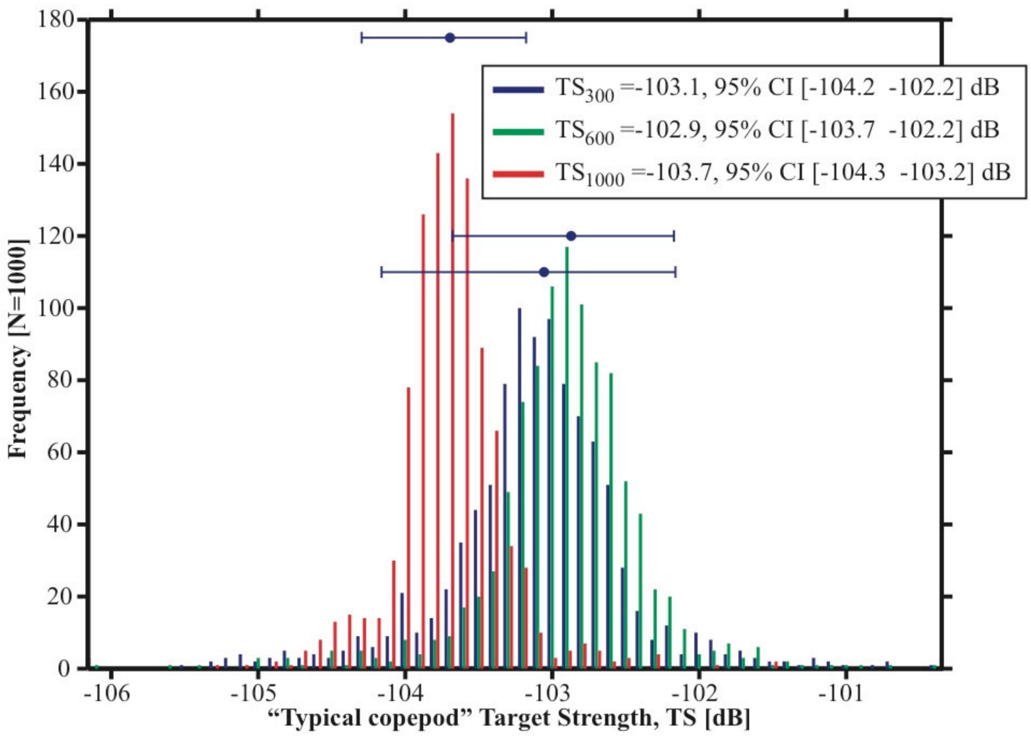

Fig. S6. Time series of depth-specific (a) cross-isobath velocity (U, m s^{-1}), (b) along-isobath velocity (V, m s^{-1}), and (c) vertical velocity (W, m s^{-1}) collected between 10 and 118 m depth using upward- and downward-looking ADCPs moored 15 m above the seafloor at the shallow-slope location on the southern margin of Roseway Basin. The white horizontal bar in each sectional plot illustrates the 4 m blanking region between the upward- and downward-looking ADCPs. Day of year (abscissa) is centered at 00:00 h ADST

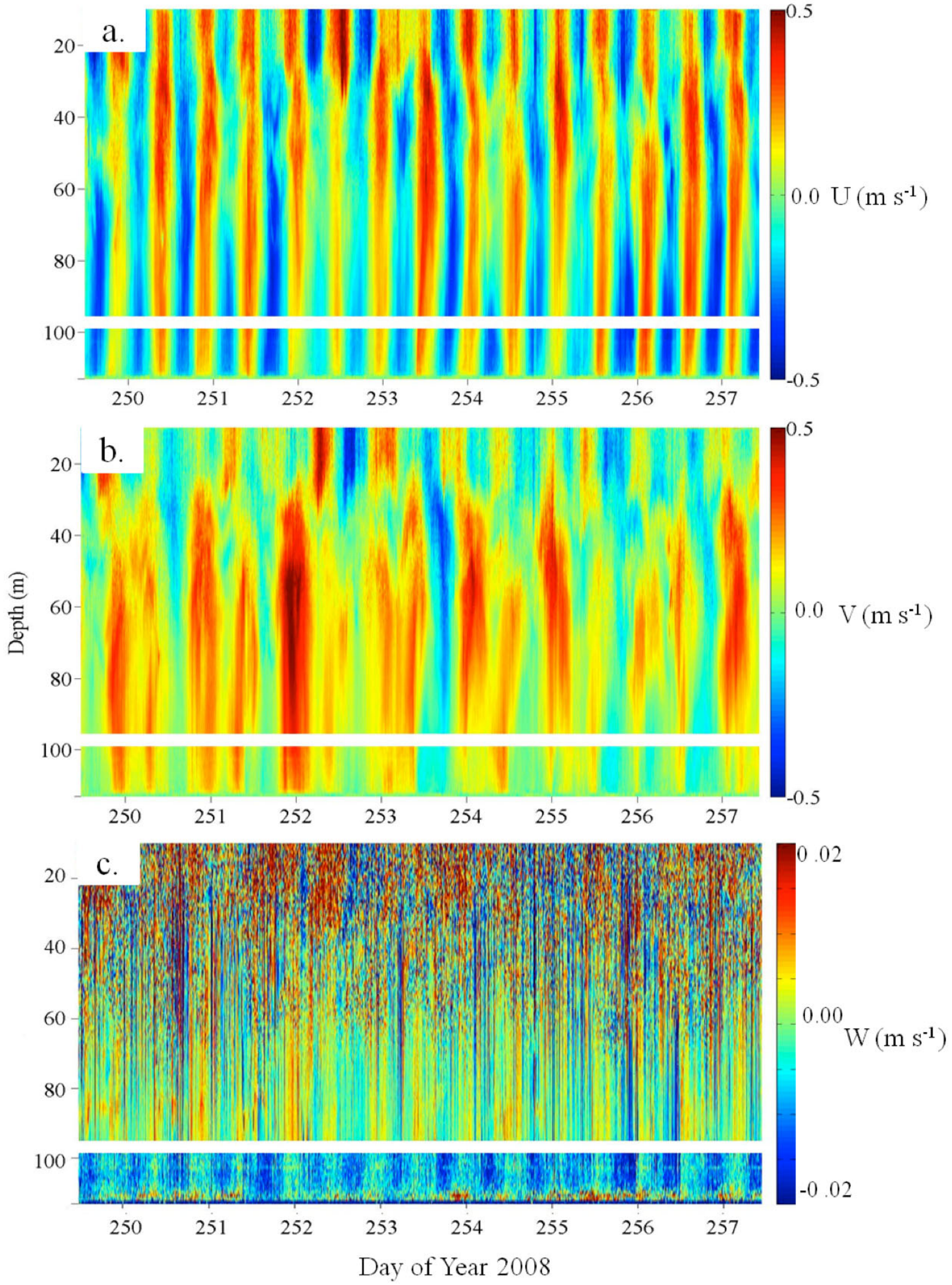

Fig. S7. As in Fig. S6, but for the deep-slope mooring

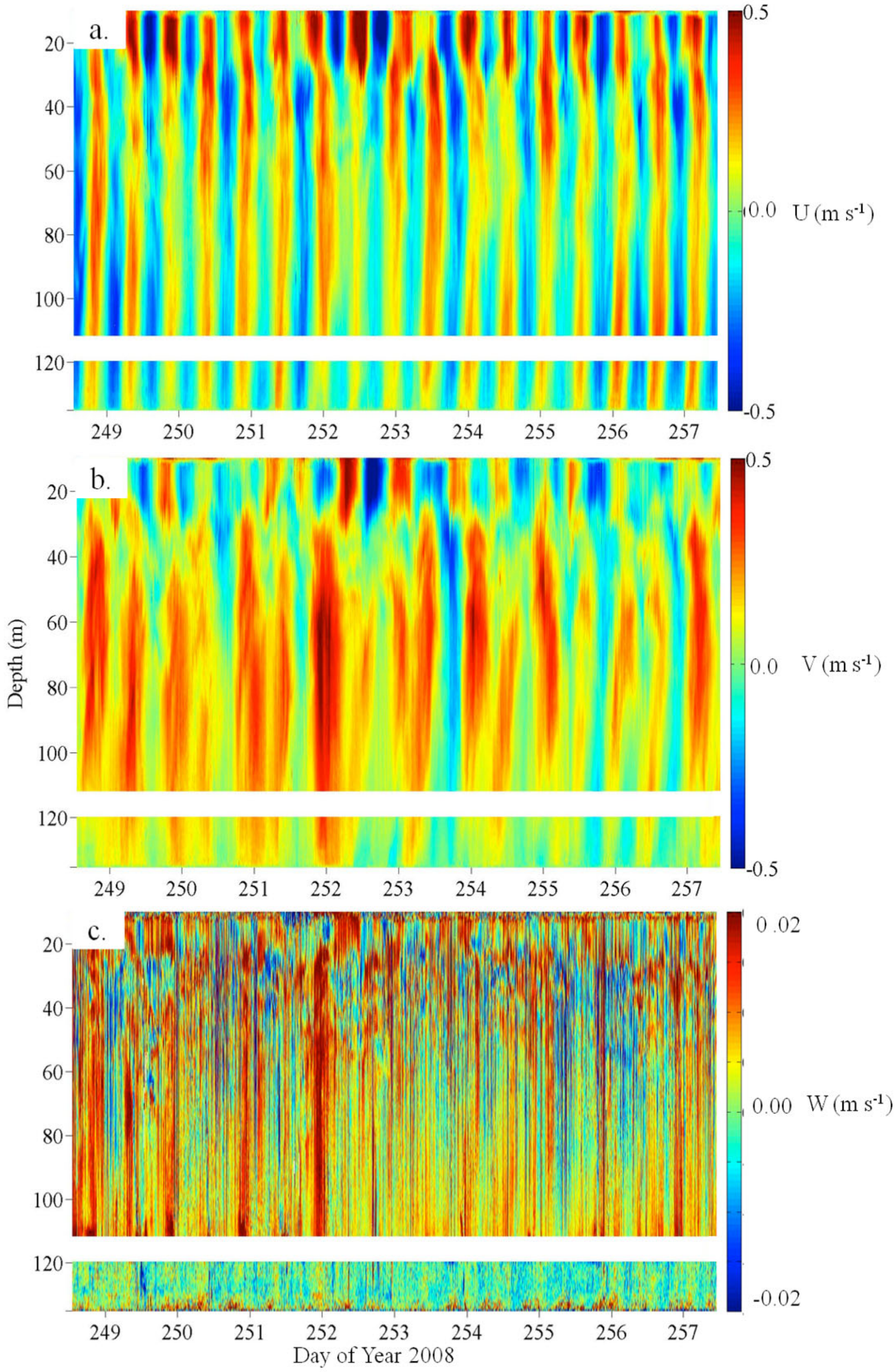

Fig. S8. Water mass density (σ_t) section aross Roseway Basin (reproduced here from Fig. 2 of the main text) used to calculate the along-isobath residual velocity generated by the density field using the thermal wind equation (Eq. S2). The black rectangle illustrates the data region used for calculations. The level of no motion was assumed at 150 m depth (dashed line). The transect line where these data were collected is illustrated in Fig. 1c in the main text

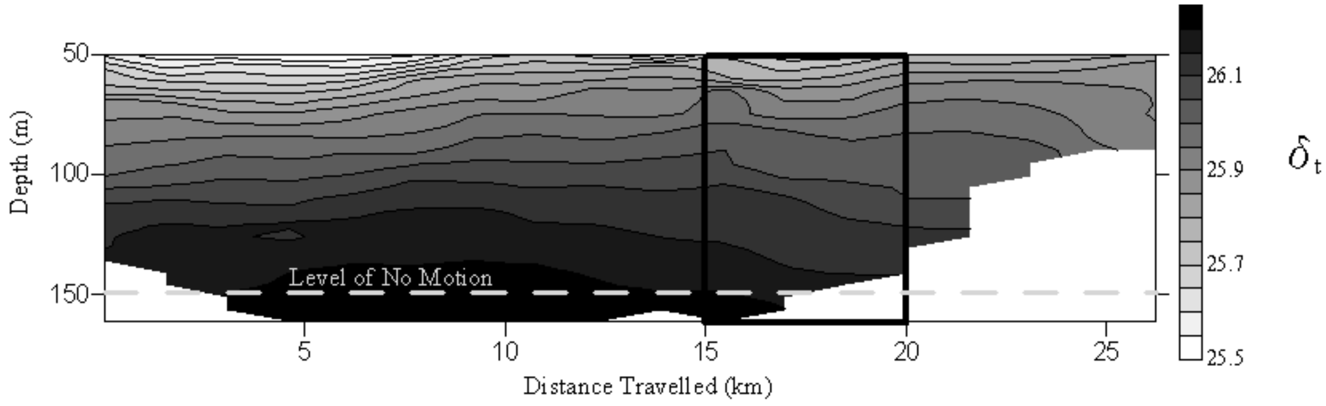

LITERATURE CITED

Deines KL (1999) Backscatter estimation using broadband Acoustic Doppler Current Profilers. Proceedings of the IEEE 6th working conference on current measurement, 1999. p 249–253

Lavery A, Wiebe PH, Stanton TK, Lawson GL, Benfield MC, Copley NJ (2007) Determining dominant scatterers of sound in mixed zooplankton populations. J Acoust Soc Am 122:3304–3326

Stanton TK, Chu D (2000) Review and recommendations for the modeling of acoustic scattering by fluid-like elongated zooplankton: euphausiids and copepods. ICES J Mar Sci 57:793–807